

# On the formation of Be stars through binary interaction

Yong Shao<sup>1</sup> and Xiang-Dong Li<sup>1,2</sup>

<sup>1</sup>*Department of Astronomy, Nanjing University, Nanjing 210093, China*

<sup>2</sup>*Key laboratory of Modern Astronomy and Astrophysics (Nanjing University), Ministry of Education, Nanjing 210093, China*

*lixd@nju.edu.cn*

## ABSTRACT

Be stars are rapidly rotating B type stars. The origin of their rapid rotation is not certain, but binary interaction remains to be a possibility. In this work we investigate the formation of Be stars resulting from mass transfer in binaries in the Galaxy. We calculate the binary evolution with both stars evolving simultaneously and consider different possible mass accretion histories for the accretor. From the calculated results we obtain the critical mass ratios  $q_{\text{cr}}$  that determine the stability of mass transfer. We also numerically calculate the parameter  $\lambda$  in common envelope evolution, and then incorporate both  $q_{\text{cr}}$  and  $\lambda$  into the population synthesis calculations. We present the predicted numbers and characteristics of Be stars in binary systems with different types of companions, including helium stars, white dwarfs, neutron stars, and black holes. We find that in Be/neutron star binaries the Be stars can have a lower limit of mass  $\sim 8M_{\odot}$  if they are formed by stable (i.e., without the occurrence of common envelope evolution) and nonconservative mass transfer. We demonstrate that isolated Be stars may originate from both mergers of two main-sequence stars and disrupted Be binaries during the supernova explosions of the primary stars, but mergers seem to play a much more important role. Finally the fraction of Be stars which have involved binary interactions in all B type stars can be as high as  $\sim 13\% - 30\%$ , implying that most of Be stars may result from binary interaction.

*Subject headings:* binaries: close – stars: emission-line, Be – stars: evolution – X-rays: binaries – X-ray: stars

## 1. Introduction

Be stars are rapidly rotating B type stars with luminosity classes III-V, which show  $H\alpha$  emission lines and excess infrared fluxes in some intervals of their lives. The characteristics of Be stars is thought to originate in the circumstellar disk (Porter & Rivinius 2003). Their rotational velocities generally reach nearly break-up velocities, leading to the formation of a gaseous decretion viscous disk around them (e.g., Lee et al. 1991; Wood et al. 1997; Okazaki 2001; Porter & Rivinius 2003; Carciofi et al. 2009; Jones et al. 2009; Sigut et al. 2009; McGill et al. 2013). The Be stars have been found either as single stars or in binary systems. In Be/X-ray binaries (BeXRBs), a compact star, usually a neutron star (NS), orbits a Be star and accretes the dense stellar wind from the Be star, therefore emitting X-rays. In the Galaxy there are 81 BeXRBs, and 48 out of them have been found to host a NS (Liu et al. 2006; Reig 2011). They have been detected as X-ray sources with luminosities in the range of  $\sim 10^{34} - 10^{38} \text{ erg s}^{-1}$ , and the orbital periods range from  $\sim 10$  days to several hundred days (Reig 2011). Recently Casares et al. (2014) discovered a Be/black hole (BH) binary MWC 656 with an orbital period  $\sim 60$  days, but its X-ray emission is extremely weak (Munar-Adrover et al. 2014). It is interesting to note that the Be stars in BeXRBs have spectral types earlier than B2 (Negueruela 1998), while isolated Be stars have a spectral distribution of A0–O9 (Slettebak 1982).

The formation of Be stars is still a controversial topic. There are three possible explanations for the origin of the rapid rotation of Be stars (e.g., Huang et al. 2010): (1) they were born as rapid rotators; (2) along the main-sequence (MS) evolution, single stars with a sufficiently high rotational velocity on the zero-age main-sequence (ZAMS) can reach equatorial velocities near the critical value, due to the transfer of angular momentum from the inner contracting part to the outer region (Ekström et al. 2008); and (3) they are the mass gainers that were spun up by a past episode of Roche-lobe overflow (RLOF) in an interacting binary (Rappaport & van den Heuvel 1982; Pols et al. 1991). During the process of RLOF, matter and angular momentum are transferred from the primary star to the secondary star, spinning up the latter to very high rotation rates (Packet 1981), which then turns into a Be star. According to McSwain & Gies (2005), about 75% of the detected Be stars may have been spun-up by binary mass transfer, while most of the remaining Be stars were likely rapid rotators at birth. Huang et al. (2010) showed that most young B type stars have rotational velocities that are well below the limit for Be star formation, suggesting that only a small fraction of Be stars were born as rapid rotators.

Using a binary population synthesis (BPS) method, Pols et al. (1991) investigated the

formation of Be stars by case B mass transfer<sup>1</sup>, and presented a comparison between the predicted number of Be stars and observations. They concluded that no more than 60% of the population of Be stars can be produced by close binary interaction. Pols et al. (1991) also attempted to address the observed lower mass limit of  $\sim 8M_{\odot}$  for the Be stars in BeXRBs, corresponding to the spectral type B2. They suggested that only systems with initial mass ratios (i.e., the ratio of the secondary mass and the primary mass) larger than 0.3 – 0.5 can produce Be stars. The argument was that systems with smaller initial mass ratios do not transfer any mass stably but evolve into a spiral-in common envelope (CE) phase, without forming Be stars. Thus Be stars with spectral type later than B2 can be effectively removed. In the calculations, they adopted a simple assumption that the supernova (SN) explosion of the primary is spherically symmetric, which helps the survival of the binary after the SN.

Portegies Zwart (1995) considered the effect of an asymmetric SN explosion and used a constant value for the kick velocity. Although the number of late-type Be stars with a NS companion is reduced slightly, the spectral distribution of the Be stars was found not to match the observations. The author then introduced possible mass loss from the binary system at the second Lagrangian point  $L_2$  during the mass transfer processes, with the escaped matter taking away  $\sim 6$  times the specific angular momentum of the binary system. Because of the high rate of angular momentum loss, the systems with small initial mass ratios would also undergo spiral-in and evolve towards a CE phase. Therefore Be stars with a NS companion should be more massive than  $\sim 8M_{\odot}$ . Van Bever & Vanbeveren (1997) also made population synthesis calculation on the formation of Be stars via binary evolution in the Galaxy and the Magellanic Clouds, incorporating updated data of the SN kick. They assumed that a minimal initial mass ratio  $q_{\min} = 0.2$  for stable mass transfer, below which CE evolution will occur. Consequently the Be stars evolved from close binary evolution were shown to contribute not too much to the total population of Be stars (less than 20% and possibly even as low as 5%). A more recent BPS study of Galactic BeXRBs was performed by Belczynski & Ziolkowski (2009), who attempted to explain the problem of the missing BeXRBs with BHs at that time. However, the discovery of MWC 656 suggests that the population of Be/BH binaries are not negligible in the Galaxy.

As mentioned above, the critical mass ratio  $q_{\text{cr}}$ , which is used to determine whether a binary system experiences stable mass transfer, is one of the vital factors in the formation of the Be stars through binary interaction. It depends closely on the structure of the donor, the nature and the mass of the accretor, and how conservative the mass

---

<sup>1</sup>The case of the mass transfer is a classification of the mass transfer by the evolutionary status of the donor: Case A - core hydrogen burning, Case B - shell hydrogen burning, Case C - after exhaustion of core helium burning.

transfer is (e.g., Podsiadlowski et al. 1992, 2002; Kalogera & Webbink 1996; Soberman et al. 1997; Li & van den Heuvel 1997; Tauris et al. 2000; Han et al. 2002; Ivanova & Taam 2004; Ge et al. 2010; Woods et al. 2012; Shao & Li 2012). Constant values or empirical formulae for  $q_{\text{cr}}$  are usually adopted in the BPS calculations. In this work we numerically calculate the critical mass ratios for various initial conditions, and use them as input in the simulations of binary evolutions that form Be stars. de Mink et al. (2013) recently investigated the evolution of the rotation rates of massive stars, and concluded that mass transfer and mergers are the main cause of rapid rotation for massive stars. Here we focus on the formation of Be stars, following some of their treatments on binary interaction, especially the processes of mergers. We introduce the calculating method and the input parameters in Section 2. In Section 3 we present the calculated results on the properties of Be stars both in binaries and as single stars, and compare them with observations. We discuss the fraction of Be stars in B type stars contributed by binary evolution and conclude in Section 4.

## 2. Method

### 2.1. The binary population synthesis code

We adopt the BSE code initially developed by Hurley et al. (2000, 2002) and revised by Kiel & Hurley (2006) to calculate the evolution of a large population of massive stars. We follow Belczynski et al. (2008) to update some of the treatments of the processes that lead to the formation and evolution of compact objects. In addition, we have modified the code in the following aspects.

We adopt the rapid supernova (SN) mechanism (Woosley et al. 2002; Fryer et al. 2012) to obtain the mass of a NS/BH after a SN explosion, which seems to account for the combined mass distribution of NSs and BHs, with a dearth of the remnants of mass between  $\sim 2M_{\odot}$  and  $\sim 4 - 5M_{\odot}$  (Ozel et al. 2010; Farr et al. 2011). The final mass of a compact object is determined by the CO core mass at the time of explosion, which gives the proto-compact object mass. In the subsequent explosion, accretion of the fallback material increases its mass to form a NS or BH. For electron-capture SNe, we apply the criterion suggested by Fryer et al. (2012) as follows. If the core mass at the base of asymptotic giant branch is between  $1.83M_{\odot}$  and  $2.25M_{\odot}$ , the CO core non-explosively burns into an ONe core and the core mass increases gradually. If the core mass can reach  $1.38M_{\odot}$ , the core collapses by electron capture into Mg and forms a NS. If the ONe core mass is less than  $1.38M_{\odot}$ , it leaves an ONe WD.

The natal kick imparted on the newborn compact objects is an important factor that

determines the formation efficiencies of XRBs. We adopt a Maxwellian distribution for the kick velocity with  $\sigma = 265 \text{ km s}^{-1}$  (Hobbs et al. 2005) for NSs formed from core-collapse SNe. For electron-capture SNe, we take a lower kick velocity with  $\sigma = 50 \text{ km s}^{-1}$  (Dessart et al. 2006). For BHs, if the fallback material fraction  $f_{\text{fb}} = 1$  (i.e., direct collapse), there is no natal kick. Otherwise we use the NS kick velocity reduced by a factor of  $(1 - f_{\text{fb}})$  for  $f_{\text{fb}} < 1$  (Fryer et al. 2012).

If the mass transfer is dynamically unstable during the ROLF, a binary will enter the CE phase. We use the standard energy conservation equation (Webbink 1984) to deal with the CE evolution,

$$\alpha_{\text{CE}} \left( \frac{GM_{1,\text{f}}M_2}{2a_{\text{f}}} - \frac{GM_{1,\text{i}}M_2}{2a_{\text{i}}} \right) = -E_{\text{bind}}, \quad (1)$$

and

$$E_{\text{bind}} = -\frac{GM_{1,\text{i}}M_{1,\text{env}}}{\lambda R_{1,\text{lobe}}}, \quad (2)$$

where  $M_1$  and  $M_2$  are the primary (mass donor) and secondary (mass gainer) masses respectively,  $a$  is the orbital separation of the binary,  $M_{1,\text{env}}$  is the mass of the primary’s envelope that is ejected from the system during the CE evolution,  $R_{1,\text{lobe}}$  is the RL radius of the primary at the onset of RLOF, and the indices i and f refer to the initial and final stages of the CE evolution, respectively. The parameter  $\lambda$  includes the effect of the mass distribution within the envelope and the contribution from the internal energy (de Kool 1990; Dewi & Tauris 2000), and  $\alpha_{\text{CE}}$  is the CE efficiency with which the orbital energy is used to unbind the stellar envelope. We employ the results in Xu & Li (2010) to calculate  $\lambda$ , and take  $\alpha_{\text{CE}} = 1.0$  in our calculations.

## 2.2. The critical mass ratio

The critical mass ratio  $q_{\text{cr}}$  can be used to determine whether the mass transfer is dynamically unstable in a binary. Instead of using the empirical results in Hurley et al. (2002) we numerically calculate the values of  $q_{\text{cr}}$  and incorporate them into the BPS code. Note that in this work we define the mass ratio  $q = M_1/M_2$ , different from in previous studies.

We use an updated version of the stellar evolution code developed by Eggleton (1971, 1972) (see also Pols et al. 1995; Yakut & Eggleton 2005) to calculate the binary evolution, and search the parameter space for stable mass transfer. In these calculations, we adopt the TWIN mode in which the structure and the composition equations for both stars, as well as the orbital properties such as the eccentricity and orbital angular momentum, are solved simultaneously. The initial chemical compositions are set to be  $X = 0.7$  and  $Z = 0.02$ . We

take the ratio of the mixing length to the pressure scale height to be 2.0, and the convective overshooting parameter to be 0.12 (Schröder et al. 1997). For the wind mass loss rates from massive stars, we take the empirical formula for luminous stars suggested by de Jager et al. (1988).

### 2.2.1. The models of mass transfer

All of the binary stars considered here initially consist of two ZAMS stars. The effective radius  $R_{L,1}$  of the primary’s RL is given by (Eggleton 1983)

$$\frac{R_{L,1}}{a} = \frac{0.49q^{2/3}}{0.6q^{2/3} + \ln(1 + q^{1/3})}. \quad (3)$$

We assume that the initial binary orbit is circular (King 1988), and the orbital angular momentum is

$$J_{\text{orb}} = \frac{M_1 M_2}{M_T} \omega a^2, \quad (4)$$

where  $M_T = M_1 + M_2$  is the total mass, and  $\omega = \sqrt{GM/a^3}$  is the orbital angular velocity.

In order to follow the evolution of the orbit and spins of the two stars in a binary, we consider the orbital angular momentum and the spin angular momentum of each binary component. We assume that the rotation of the stars is rigid. The coupling of the orbit and the spins is controlled by tidal interaction, and we account for the spin-orbit interaction by using the equilibrium tide theory (Hut 1981). The code includes the loss of angular momentum by stellar winds and the transfer of angular momentum between the two stars.

As RLOF occurs, mass transfer onto the secondary will cause it to expand and spin up. The secondary is also rejuvenated due to accretion (Hurley et al. 2002). Several authors (e.g., Ulrich & Burger 1976; Neo et al. 1977; Pols & Marinus 1994) have investigated the evolution of accreting MS stars and obtained the following results. If the mass transfer time scale  $\tau_{\dot{M}} (= -M_1/\dot{M}_1$ , where  $-\dot{M}_1$  is the mass transfer rate) is longer than the thermal time scale  $\tau_{KH2}$  of the accretor, the mass transfer is stable, and the mass gainer can remain in thermal equilibrium. On the other hand, if  $\tau_{\dot{M}} < \tau_{KH2}$ , the accretor will get out of thermal equilibrium and expand. This expansion may finally cause the accretor to fill its own RL, leading to the formation of a contact binary (e.g., Nelson & Eggleton 2001). The conditions for thermal-timescale RLOF imply that the donor is more massive than the accretor and possesses a radiative envelope, i.e., mass transfer occurs in case A or early case B phases. Dynamically unstable mass exchange usually occurs when the donor has developed a deep convective envelope, i.e., mass exchange in late case B or case C phases.

Packet (1981) pointed out that only a small amount of accreted mass can spin up the accretor to critical rotation. It is still unclear whether and how a rapidly rotating star can keep accreting mass. Petrovic, Langer & van der Hucht (2005) and de Mink et al. (2009) assumed that mass accretion ceases when the accretor reaches the critical rotation. Alternatively, de Mink et al. (2013) suggested that a star can continue to accrete even with the critical rotation, based on the argument of Paczynski (1991) and Popham & Narayan (1991) that the accretion disk can regulate the mass and angular momentum flux through viscous coupling.

In summary, mass accretion can spin up the accretor, cause it to expand, and probably result in mass loss. Since the process is rather complex, here we construct three models to investigate the stability of mass transfer, using the Eggleton’s code to follow the response of the accretor.

*Model I: rotation-dependent mass accretion*

We adopt the suggestion by Stancliffe & Eldridge (2009) to deal with the accretion of rapidly rotating stars. It is assumed that the accretion rate onto a rotating star is reduced by a factor of  $(1 - \Omega/\Omega_{\text{cr}})$ , where  $\Omega$  is the angular velocity of the star and  $\Omega_{\text{cr}}$  is its critical value. In this model a star rotating at  $\Omega_{\text{cr}}$  will not accrete mass anymore, and we assume that the remaining material is ejected out of the binary in the form of isotropic wind, carrying the accretor’s specific orbital angular momentum  $j_{\text{iso}} = (M_1/M_2)(J_{\text{orb}}/M_{\text{T}})$ .

*Model II: half mass accretion and half mass loss*

We do not consider the detailed effects of rotation, and assume that half of the transferred mass is accreted by the secondary, and the other half is lost from the system, also taking the specific orbital angular momentum of the accretor (see also de Mink et al. 2007).

*Model III: thermal equilibrium limited mass accretion*

In this case we assume that the transferred mass is always accreted by the secondary unless its thermal timescale becomes much shorter than the mass transfer timescale. Specifically, the accretion rate is assumed to be limited by  $-\left[\min\left(10\frac{\tau_{\dot{M}}}{\tau_{KH2}}, 1\right)\right]\dot{M}_1$  (Hurley et al. 2002). Rapid mass accretion may drive the accretor out of thermal equilibrium, which will expand and become overluminous. In our calculations, the values of  $\tau_{KH2}$  are found to be usually much lower than that of the same star in thermal equilibrium, so that  $\tau_{KH2} < 10\tau_{\dot{M}}$  always holds, meaning that mass transfer is generally conservative.

Note that Models I and III represent two extreme cases of mass transfer, corresponding to highly non-conservative [only a small fraction ( $\lesssim 10\%$ ) of the transferred material is accreted by the secondary] and roughly conservative mass transfer, respectively. Model II

describes an intermediate between them, with 50% of the transferred mass accreted.

In our calculations the binary evolution will be stopped when either the radius of the accretor exceeds its RL radius or the mass transfer rate rises rapidly to very high rate ( $> 10^{-3} M_{\odot}\text{yr}^{-1}$ ) and the code fails to converge. The binary is then assumed to become contact or enter the CE phase. The evolution of contact binaries, however, is not yet fully understood. It may be driven not only by mass transfer but also by luminosity transfer between the components (Shu & Lubow 1981). We follow the previous suggestion that the fate of contact binaries consisting of two MS stars is a merger, forming a single star with rapid rotation (de Mink et al. 2007, 2013; Jiang et al. 2013). For the contact binaries containing a Hertzsprung gap (HG) donor, de Mink et al. (2013) assumed that they will merge to become blue or red supergiants. Here we assume that they will evolve into the CE phase following Hurley et al. (2002), and whether the binary components will merge is determined by the energy equation in Section 2.1.

### 2.2.2. *The parameter space for stable mass transfer*

We have calculated the mass transfer processes in a grid of binaries with different values of the initial parameters. The primary masses  $M_1$  are taken to be 1.5, 3, 5, 7, 10, 20, 30, 40, 50, and  $60 M_{\odot}$ . The orbital periods  $P_{\text{orb}}$  (in units of days) vary logarithmically from  $-0.5$  to  $3.5$  by steps of  $0.1$ . If the initial orbital period is so short that the primary has filled its RL at the beginning of binary evolution, it will skip to the next longer orbital period. The mass ratios  $q$  are increased from  $1.2$  to  $6$  by steps of  $0.2-0.5$ .

In Fig. 1 we outline the boundaries that determine whether a binary can evolve successfully with stable mass transfer in the initial  $P_{\text{orb}} - M_1$  plane. The left, middle and right panels correspond to the results in Models I, II and III, respectively. The values of initial  $q$  are indicated with different colors in the figure. The solid curves, which always appear in pairs, show the lower and upper boundaries of the parameter space for a specific  $q$ , between which the mass transfer can proceed stably. We also plot other curves to distinguish the evolutionary states of the donor star - the thick grey curve (which overlaps with the curves for the upper boundary in the left panel) denotes the orbital periods when the primary fills its RL at the end of HG; the green dashed and dotted curves represent the orbital periods when the RL-filling primary is at the beginning and at the end of MS, respectively.

We see from Fig. 1 that the mass transfer always becomes runaway when the primary has climbed to the (super)giant branch and developed a deep convective envelope prior to the mass exchange. In Model I, expansion of the mass gainer is not significant because of small

amount of mass accreted. Loss of mass and angular momentum from the binary shrinks the orbit before the mass ratio reverses. For a binary with sufficiently short  $P_{\text{orb}}$ , this may lead to the accretor’s radius exceeding its RL radius. The value of  $q_{\text{cr}}$  for stable mass transfer can reach as high as  $\sim 6$ . In Model II, half of the transferred material is assumed to leave the binary. The regions for stable mass transfer seem to be odd, with isolated “islands” in the parameter space in some cases, implying that the stability of the mass transfer is sensitive to the orbital periods and the masses of the binary components. Generally  $q_{\text{cr}} \lesssim 2.5$  in this case. In Model III the secondary accretes more material from the primary than in Models I and II, and expands more significantly, so the parameter space for stable mass transfer without contact is smaller. We can see that for a HG star with  $M_1 \gtrsim 20M_{\odot}$ , a contact phase always occurs. In this situation  $q_{\text{cr}} \lesssim 2.2$ . Generally the lower the mass ratio, the bigger the allowed parameter space is. In the appendix we present two examples of the evolutionary tracks, to demonstrate how the mass transfer depends on the initial parameters and mass loss modes.

### 2.3. Possible channels to form a Be star

Although Be stars are thought to be rapidly rotating B type stars, it is controversial how fast a B star can spin before it becomes a Be star. To calculate the number and distribution of Be stars in the Galaxy, we adopt a phenomenological definition of Be stars based on their observational spectral types and characteristics, i.e., they are MS stars of mass between  $3 M_{\odot}$  and  $22 M_{\odot}$ , rotating at  $\geq 80\%$  of their break-up velocities  $V_{\text{cr}}$  (Slettebak 1982; Negueruela 1998; Porter & Rivinius 2003).

Here we consider the binary interaction to form Be stars involving stellar winds, tides, mass transfer and mergers (see also de Mink et al. 2013). We follow the treatments on these processes in Hurley et al. (2002) and Kiel & Hurley (2006) to calculate the stellar rotation in binary systems.

*Stellar evolution.* When there is angular momentum transfer between the inner and outer parts of a star, the stellar rotation is decided by the stellar structure. The moment of inertia of the star,  $I = kMR^2$ , where  $k$  is the radius of gyration squared, is given by Pols in form of fitting formulae (see de Mink et al. 2013), and added in the BSE code. For ZAMS stars, the gyration radius squared  $k_0$  is given by

$$k_0 \simeq c + \min\{0.21, \max(0.09 - 0.27 \log M, 0.037 + 0.033 \log M)\}, \quad (5)$$

where  $c = -0.055(\log M - 1.3)^2$  for  $\log M > 1.3$ , otherwise  $c = 0$ . When a star evolves along the MS, its outer layers tend to expand as the core contracts. The value of  $k$  can be

described as a function of the current radius  $R$  and the radius  $R_0$  at ZAMS,

$$k \simeq (k_0 - 0.025) \left( \frac{R}{R_0} \right)^\alpha + 0.025 \left( \frac{R}{R_0} \right)^{-0.1}, \quad (6)$$

where

$$\alpha = \begin{cases} -2.5 & \log M < 0, \\ -2.5 + 5 \log M & \text{for } 0 < \log M < 0.2, \\ -1.5 & 0.2 < \log M. \end{cases} \quad (7)$$

The internal rotational profile of a star is set to be rigid rotation in the BSE code, same as in de Mink et al. (2013).

*Tidal interaction.* Tidal torques in binary stars tend to synchronize the stellar rotation with the orbital motion. The efficiency is critically dependent on the ratio of the stellar radius to the binary separation (Zahn 1977; Hut 1981), and the effect of tides is strong in short-period systems. If the synchronization time scale is less than the MS lifetime of the Be star, the Be star may synchronize its rotation with the orbital motion, losing its Be character before leaving the MS (Raguzova & Lipunov 1998). This will reduce the formation rate of Be stars in narrow systems.

*Mass transfer.* We follow the treatment of de Mink et al. (2013) on the transfer of mass and angular momentum. During RLOF the transferred material may either form an accretion disk around the secondary or directly impact on its surface, depending on the minimum distance  $R_{\min}$  compared with the accretor’s radius  $R_2$  (Lubow & Shu 1975). If the  $R_{\min} < R_2$ , the stream impacts directly on its surface, and the specific angular momentum of the impact stream is  $\sim (1.7GM_2R_{\min})^{1/2}$ . Otherwise the mass flow misses the accretor and collides with itself at a larger radius, after which the viscous process leads to the formation of a Keplerian accretion disk. The inner edge of the accretion disk will stretch inward until contact with the surface of the star, and the specific angular momentum of the transferred matter can be expressed as  $(GM_2R_2)^{1/2}$ .

There are two types of mass transfer processes associated with the Be star formation: the mass transfer without the CE occurrence and the post-CE mass transfer<sup>2</sup>. The former (termed as channel 1) has been discussed by some authors (Pols et al. 1991; Portegies Zwart 1995; Van Bever & Vanbeveren 1997). When the primary overflows its RL, if the mass transfer proceeds stably and a CE stage is avoided, transfer of matter will be able to spin up the secondary to be a Be star; the remnant of the primary will evolve to be a helium

---

<sup>2</sup>The pre-CE mass transfer and CE evolution usually proceed so rapidly that the secondary hardly accretes any matter.

burning star (He star), and finally a compact object (WD, NS or BH). The latter (termed as channel 2) involves the CE evolution. If the system survives the spiral-in phase, the left binary will contain a He star and a MS star. The He star then evolves and fills its RL once more, and transfers material to the secondary, leading to the formation of a Be star (Belczynski & Ziolkowski 2009).

*Mergers of two MS stars.* Unstable mass transfer will cause the binary to enter a CE stage or come into contact and coalescence. For CE evolution, if the orbital energy is not enough to unbind the primary’s envelope, the secondary will merge into the primary. If the two MS stars become contact, the binary is also assumed to merge into a MS star<sup>3</sup>. We follow Hurley et al. (2002) to account for the products of mixing and mergers. After the merger, the product will settle into thermal equilibrium on a thermal timescale and we assume that it can efficiently lose the excess angular momentum, forming a fast rotating star. However, the original prescription of Hurley et al. (2002) assumes that the product of mergers involving two MS stars is completely mixed and no mass is lost during this process. This may underestimate the convective core mass for massive post-merger MS stars. Here we assume that a certain fraction  $\mu_{\text{loss}}$  of the total mass of the binary system is lost during the merger. In our calculation,  $\mu_{\text{loss}} = 10\%$  is adopted, in line with Lombardi et al. (1995) and de Mink et al. (2013).

### 3. Results

The evolution of a primordial binary is determined by four initial parameters: the primary mass  $M_1$ , the secondary mass  $M_2$ , the separation  $a$  (or orbital period  $P_{\text{orb}}$ ), and the eccentricity  $e$ . The initial eccentricity has minor effect on the population synthesis results (Hurley et al. 2002), thus we assume circular orbits here for simplicity. In our calculations, the masses of the primary are chosen to be in the range of  $1.5M_{\odot}$  to  $60M_{\odot}$ , since the remnants of stars with  $M_1 \geq 60M_{\odot}$  are extremely rare according to the initial mass function (IMF). The secondary masses are set to be between  $0.1M_{\odot}$  and  $25M_{\odot}$  to ensure that almost all of the Be stars are contained, with a flat distribution of  $1/q$ . For the initial orbital separation, we assume that  $\ln a$  is evenly distributed between  $a = 3R_{\odot}$  and  $10^4R_{\odot}$ . We adopt solar metallicity  $Z = 0.02$  and an IMF with a power-law exponent of  $-2.7$  (Kroupa et al. 1993). A constant star formation rate ( $S = 5M_{\odot} \text{ yr}^{-1}$ ) is assumed over the past 15 Gyr.

In Table 1 we present the calculated numbers of binaries containing a Be star with a

---

<sup>3</sup> Stars evolved off the MS stage have developed a core in its center, and the product of the merged binary will remain this core so that it does not belong to a Be star.

He star/WD/NS/BH companion ( $N_{\text{BeHe}}$ ,  $N_{\text{BeWD}}$ ,  $N_{\text{BeNS}}$ , and  $N_{\text{BeBH}}$ , respectively), and of isolated Be stars originating from disrupted Be/NS and Be/BH systems, and from mergers of two MS stars ( $N_{\text{dBeNS}}$ ,  $N_{\text{dBeBH}}$  and  $N_{\text{merger}}$ , respectively) in the Galaxy. We see that the numbers of Be binaries drop significantly with the increasing mass of the compact stars. The value of  $N_{\text{BeHe}}$  varies drastically from  $\sim 10^5$  (channel 1) to  $< 100$  (channel 2), suggesting that very few Be/He systems can be produced after the CE evolution. The number from mergers of two MS stars is zero in channel 2, because this situation does not happen at all. Detailed results on the formation of Be stars are described below.

### 3.1. Be/NS binaries

The formation of Be/NS binaries has been investigated by many authors (e.g., Rappaport & van den Heuvel 1982; van den Heuvel & Rappaport 1987; Pols et al. 1991; Portegies Zwart 1995; Van Bever & Vanbeveren 1997; Raguzova 2001; Belczynski & Ziolkowski 2009). There are 81 confirmed BeXRBs in our Galaxy, and 48 of them host a NS (Liu et al. 2006; Reig 2011). For most of them the spectral types of Be stars and the orbital periods are known (Negueruela 1998; McBride et al. 2008), so we can compare the calculated results with the observations, and present possible constraints on the formation processes of BeXRBs.

Figure 2 shows the distribution of the masses ( $M_{\text{Be}}$ ) of Be stars in Be/NS binaries in the blue solid lines. The grey solid lines represent the distribution derived from observations (data are taken from Reig 2011). The left, middle and right panels correspond to the results with Models I, II and III, respectively. For each model, the top and bottom panels reflect the results from channels 1 and 2, respectively. The blue dashed lines denote the accretion fraction  $f$ , i.e., the ratio of the average accreted masses over stars in each bin and the Be star mass.

We first discuss the distribution of  $M_{\text{Be}}$  in the top panels obtained from channel 1. The Be stars hardly accrete any more material after reaching the break-up limit in Model I, so  $f \lesssim 0.1$ , and a large fraction of the Be stars tend to have relatively low mass. In Model II, the Be stars can accrete half of the transferred mass from the donor, so  $M_{\text{Be}} \gtrsim 8M_{\odot}$  and  $f \sim 0.3 - 0.5$ . In Model III, more mass can be accreted, thus  $M_{\text{Be}} \gtrsim 13M_{\odot}$  and  $f \gtrsim 0.45$ . From Model I to Model III, the parameter space for stable mass transfer becomes smaller, the fraction of accreted material becomes larger, hence the predicted numbers of Be/NS binaries reduce from  $\sim 1800$  to  $\sim 100$ , and the minimal masses of the Be stars increase from around  $3M_{\odot}$  to around  $13M_{\odot}$ . The distributions of  $M_{\text{Be}}$  in the bottom panels (from channel 2) are roughly similar, ranging from around  $3M_{\odot}$  to around  $10 - 13M_{\odot}$ . The main reason is that, after CE evolution, the remaining He star is generally less massive than the accretor,

so the transferred matter is relatively small, and  $f < 0.2$  always holds for the three models. Obviously the predicted distribution of Be/NS binaries through channel 1 of Model II seems to best fit the observations.

Figure 3 shows the  $P_{\text{orb}}$  distributions in the three models for systems formed through channels 1 and 2, respectively<sup>4</sup>. The observational orbital periods of the BeXRBs in the Galaxy lie in the range of  $\sim 10 - 300$  days (e.g., Belczynski & Ziolkowski 2009; Cheng et al. 2014, and references therein), more compatible with the results from channel 1.

It is well known that the spectral types of isolated Be stars in our Galaxy can be late than A0 (corresponding to  $\sim 3 M_{\odot}$ ), but in BeXRBs the Be stars are more massive than  $\sim 8 M_{\odot}$  (Negueruela 1998; McBride et al. 2008). In order to explain this difference, Pols et al. (1995) assumed that evolution of a close binary with initial mass ratio larger than 2.5 would not produce any Be stars, because they do not transfer any mass but rather evolve towards a CE phase. Portegies Zwart (1995) instead suggested mass loss from the  $L_2$  point in binary systems. The basic idea is that the related effective angular momentum loss can promote the binary to evolve into a CE stage, and only binaries with  $M_2 > 8 M_{\odot}$  can survive. In our approach, we have taken into account both the mass transfer stability and the possible effect of mass loss under different conditions. We find that only in channel 1 of Model II, the calculated mass distribution of Be stars is in line with observations, but for Be/NS binaries formed from channel 2 of the same model, the distributions of both  $M_{\text{Be}}$  and  $P_{\text{orb}}$  disagree with the observation<sup>5</sup>. We will address this issue below.

Huang et al. (2010) found that the lowest velocity that a star has to reach to show the Be-effect may vary as a function of the stellar mass. Low-mass ( $< 4 M_{\odot}$ ) B stars need to rotate extremely fast ( $V_{\text{eq}}/V_{\text{cr}} \gtrsim 0.96$ , where  $V_{\text{eq}}$  is the rotational velocity at the equatorial plane) to create an outflowing disk, while for massive stars ( $> 8.6 M_{\odot}$ ), the threshold drops to  $V_{\text{eq}}/V_{\text{cr}} \sim 0.63$ . In Fig. 4 we plot the number distributions of Be/NS systems in Model II as a function of  $M_{\text{Be}}$ , with the black and red curves corresponding to the threshold value of  $V_{\text{eq}}/V_{\text{cr}} = 0.8$  and  $0.95$ , respectively. We find that, with a higher  $V_{\text{eq}}/V_{\text{cr}} = 0.95$ , the number of low- and intermediate-mass Be stars can be reduced slightly, but there are still too many such Be/NS binaries. The reason is that a star can be spun up to critical rotation

---

<sup>4</sup>In Fig. 3,  $P_{\text{orb}}$  is cut off at the maximal orbital period of 1000 days, because Be/NS systems with longer periods may not be observed as XRBs due to the very low accretion luminosity.. The orbital periods of Be/NS binaries in channel 1 are mainly distributed around  $10 - 1000$  days (the solid lines), while those in channel 2 have relatively shorter periods, peaked around a few days to tens of days (the dashed lines), because of orbital shrink during the CE phase

<sup>5</sup>We need to caution that the observed limit of about  $8 M_{\odot}$  is affected by the rather uncertain mass determination of Be stars, as well as by possible incompleteness of the observed sample of BeXRBs.

by accreting about (10 – 15)% of its original mass (Packet 1981), and this can be practically satisfied by most post-CE mass transfer.

Here we propose two possible ways to remove intermediate-mass Be stars in Be/NS systems. (1) To form a Be star, there should be enough mass accreted by the secondary star with  $f > 0.2$ . When calculating the stellar rotation, we assumed that the star is rigidly rotating, while differential rotation may be more realistic. In addition, when the accretor spins up to close to the critical limit, it may lose mass due to the effect of the centrifugal force (Petrovic, Langer & van der Hucht 2005). Thus more accreted mass is needed to turn a B type star into a Be star. The accreted mass during the post-CE mass transfer process is relatively small with  $f$  always  $< 0.2$ . If this threshold works, then low- and intermediate-mass Be stars would not be produced in this channel. (2) The effect of magnetic braking combining strong magnetic field (as in Bp stars) and the enhanced wind could spin down the stars. This model was established by Dervişoğlu et al. (2010) and Deschamps et al. (2013) for the spin angular momentum evolution of the accretors in Algol-type binary stars. A differentially rotating star might generate magnetic fields in its radiative atmospheres. The processes of accretion may also induce strong winds which interacts with the magnetic field ( $\gtrsim 1$  KG). Due to magnetic braking, the rotational velocity of the accretor may be reduced to below its critical limit and lose the character of a Be star. The problem with this explanation is that no magnetic field has been reliably detected in any Be star (Wade et al. 2012).

Based on the above arguments we do not favor the formation of Be/NS binaries through the post-CE mass transfer. In the following we only discuss the Be stars formed through channel 1. As the mass distribution of Be stars in Be/NS binaries can fit the observation better in Model II, we regard it as the standard model and discuss the results in this model in the following, if not mentioned otherwise. However, we note that the assumption of 50% accretion efficiency in Model II is completely ad hoc, and Models I and III are actually more physical, considering the roles of rotation and thermal equilibrium of the accretor to constrain the accretion processes. The fact that Model II can better reproduce the BeXRB population indicates that some important physics is still lacking in the treatment of the binary evolution. Meanwhile, the obtained results also depend on the adopted ways of mass loss. All the three models assume isotropic re-emission of the material that is not accreted.

Figure 5 displays the expected distribution of Be/NS binaries in the  $P_{\text{orb}} - e$  plane. In the left and right panels we plot the binaries with the NSs originating from electron-capture SNe and core-collapse SNe, respectively. During core-collapse SNe the newborn NSs experience violent explosions and a high-velocity kick, the resulting binaries tend to have eccentricities  $> 0.5$ . In the case of electron-capture SNe, the binary eccentricities  $\lesssim 0.7$ . The eccentricity distribution may provide important information about the two subpopulations of BeXRBs

resulting from different types of SNe (Knigge et al. 2011, see however, Cheng et al. 2014).

### 3.2. Be/BH binaries

There is currently only one confirmed Be/BH binary in the Galaxy, i.e., MWC 656 (Casares et al. 2014), which contains a BH of mass  $3.8 - 6.9M_{\odot}$  in a  $\sim 60$  day orbit. From our BPS calculations, the number of Be/BH systems is  $\sim 10$  in the standard model, but increases to  $\sim 250$  in Model I. In Model III, no Be/BH can be formed, because in the case of stable mass transfer with  $M_1 > 20M_{\odot}$ , the secondary mass has been increased to  $> 22M_{\odot}$ . Figure 6 shows the distribution of Be/BH binaries in the  $P_{\text{orb}} - M_{\text{Be}}$  plane, with the left and right panels corresponding to Models I and II, respectively (the dashed line denotes the orbital period of NWC 656). The masses of the Be stars can be as low as  $\sim 8M_{\odot}$  in Model I, while in Model II  $M_{\text{Be}} \gtrsim 18M_{\odot}$ . Belczynski & Ziolkowski (2009) have explored the formation of the populations of Be/NS and Be/BH binaries, and found the numbers of these two types of systems to be  $579 - 1578$  and  $19 - 82$ , respectively. The numbers of Be/BH systems from their calculation are covered by ours. In particular, the ratio of Be binaries with NSs to the ones with BHs is  $\sim 7 - 53$  (in Models I and II), while the preferred value is  $\sim 30 - 50$  in Belczynski & Ziolkowski (2009). The difference results from different definitions of BeXRBs and different treatments on the formation of Be stars. For example, Belczynski & Ziolkowski (2009) assumed that a constant fraction of B type stars are Be stars, and that all binaries either survive CE evolution or evolves to a merger if the donor star is in the HG.

Finally we emphasize that in both Belczynski & Ziolkowski (2009) and this work semi-analytic formulae (e.g. Fryer et al. 2012) are adopted to estimate the BH masses, which are assumed to be largely determined by the progenitor mass<sup>6</sup>. However, it has been shown that successful SN explosions are intertwined with failures in a complex pattern that is not well described by the progenitor initial mass and is not simply related to compactness (Kochanek 2014; Pejcha & Thompson 2014, and references therein). For example, progenitors with certain initial masses less than  $20 M_{\odot}$  are likely to form BHs rather NSs. This may remarkably influence the predicted number of BHs and the BH mass functions.

---

<sup>6</sup>Also note that in Eq. (16) in Fryer et al. (2012),  $a_1$  should be  $0.25 - 1.275/(M - M_{\text{proto}})$  rather  $0.25 - (1.275/M - M_{\text{proto}})$ .

### 3.3. Be/He and Be/WD binaries

Most of the Be binaries contain a He star or a WD companion (see Table 1). In Figs. 7 and 8 we plot the distributions of Be/He and Be/WD binaries in the  $P_{\text{orb}} - M_{\text{Be}}$  plane, respectively. The mass distributions of Be stars in the Be/He and Be/WD binaries are shown in Fig. 10 with red and green curves, respectively.

Our calculations show that a Be star can have a He companion with mass  $\sim 0.3 - 17M_{\odot}$ . When the He star’s mass is less than  $\sim 2.5M_{\odot}$ , the rejuvenated MS lifetime of the Be star becomes shorter than that of the He star, and such binaries contribute most to the population of Be/He binaries. During the formation of Be/compact star binaries, the primaries also spend some time in the He star stage when their envelopes are stripped, although these He stars are more massive and evolve quickly into compact stars before the Be stars evolve off the MS. The orbital periods of Be/He binaries lie between  $\gtrsim 10$  days and  $\sim 200$  days, and cluster around  $\sim 20$  days. Based on the combined energy distribution of a B2V star and a  $1M_{\odot}$  He star companion, Pols et al. (1991) showed that the luminosity of the binary in XUV should be dominated by the He star. At lower frequencies the contribution of the He star is negligible and it is difficult to detect these systems.

The orbital periods of Be/WD binaries also range from  $\sim 10$  days to  $\sim 200$  days, and peak around  $\sim 20$  days. They tend to possess intermediate-mass Be stars, similar as Be/He binaries. Raguzova (2001) found that the peak of the  $P_{\text{orb}}$  distribution is  $\sim 100$  days and there are very few systems with  $P_{\text{orb}} \lesssim 30$  days. The differences mainly result from the synchronization mechanisms adopted. In Raguzova (2001), relatively short-period Be/WD binaries are removed from the population due to the operation of the synchronization mechanism of Tassoul (1987). This mechanism is more efficient than that suggested by Zahn (1977) adopted in the BSE code, so stars with  $P_{\text{orb}} \sim 10 - 30$  days can be synchronized and lose the Be character.

Our calculations suggest that there may be  $\sim 10^5$  Be/WD binaries in the Galaxy. It is interesting to note that currently there are no Be/WD binaries observed in the Galaxy, though three were identified in the Large and Small Magellanic Clouds (Kahabka et al. 2006; Sturm et al. 2012; Li et al. 2012). The circumstellar disk of the Be star may be truncated by the tidal torque from the WD, because of its circular orbit (Artymowicz & Lubow 1994; Negueruela & Okazaki 2001; Zhang et al. 2004), with little accretion onto the WD. In this case the WD’s UV and optical emission powered by cooling could be detected for hottest WDs. If the truncation is inefficient and the WD can accrete matter from the Be star disk, it might experience episodes of shell burning (as in nova systems), appearing as a transient supersoft X-ray source. However, its XUV and soft X-ray radiation is likely to be absorbed by the gas in the envelope of the Be star in which the WD is embedded (Apparao 1991).

Analyses by Nielsen et al. (2013) and Wheeler & Pooley (2013) suggest that small amount of circumstellar matter local to the WD can easily suppress its X-ray emission.

### 3.4. Isolated Be stars

The masses of isolated Be stars can be as low as  $3M_{\odot}$  (Slettebak 1982). Here we consider their formation through binary evolution in two ways. The first is from “disrupted Be/NS and Be/BH systems” because of the SN explosions. When the primary star evolves to experience a SN explosion and leaves a NS or BH, the binary system may be disrupted and produce an isolated Be star. Be stars originating from disrupted Be/NS systems are much more numerous than from Be/BH systems (see Table 1), because of the IMF and larger amplitude kicks imparted on the NSs. The mass distributions of the calculated (in the standard model) and observed isolated Be stars are plotted in Fig. 9 in the blue and grey solid lines, respectively. The observational data were taken from Slettebak (1982) with a magnitude limit of  $V \leq 6$ , so many late-type Be stars might have been missed due to the selection effect, and the actual distribution of isolated Be stars may have a even lower mass peak. The number of isolated Be stars originating from disrupted Be/NS systems in the standard model is estimated to be  $\sim 5200$ , about 10 times the number of the surviving Be/NS systems. The masses of the Be stars are generally larger than  $\sim 8M_{\odot}$ , similar as in Be/NS systems.

The second and much more important formation channel of isolated Be stars is the merger of two MS stars. In the standard model, the number of Be stars formed through mergers is  $\sim 1.9 \times 10^6$ , similar as in Models I and III. This is much more than from the disrupted Be/NS systems. More importantly, the predicted Be stars tend to have low masses, compatible with the observation (we need to mention that in the observed sample in Fig. 9 (also in Figs. 10 and 11 below) is obviously incomplete, so we can only compare the shapes of the distributions), suggesting that mergers are more promising in forming isolated Be stars.

## 4. Discussion and conclusions

In this paper, we investigate the formation of Be stars through mass transfer and mergers in binaries. In Fig. 10 we present the mass distributions of all Be stars in binaries, and of isolated Be stars formed from disrupted Be/NS and Be/BH systems. The thick blue line reflects the overall distribution of these Be stars. For  $M_{\text{Be}} < 10M_{\odot}$ , it is dominated by Be stars with a He star and a WD companion. More massive Be stars are likely to be isolated

Be stars from disrupted Be/NS systems.

How important is binary interaction in the formation of Be stars? Since mergers of two MS stars may also produce Be stars, we compare in Fig. 11 the mass distributions of Be stars formed through channel 1 and mergers in the standard model, as well as all B type stars with the blue, green, and black lines, respectively. Their numbers are correspondingly  $\sim 5.7 \times 10^5$ ,  $\sim 1.9 \times 10^6$ , and  $\sim 1.17 \times 10^7$ . Obviously these numbers depend on the fraction of massive binaries, IMF, and the initial mass ratio distribution. The fraction of binaries in the Galaxy has been shown to be 69% ( $\pm 9\%$ ) with orbital periods between  $10^{0.15}$  days and  $10^{3.5}$  days (Sana et al. 2012; de Mink et al. 2013). So we take the binary fraction to be between 50% and 100%, and plot the calculated fraction of Be stars in B type stars in Fig. 12. Pols et al. (1991) concluded that no more than 60% of the population of Be stars are formed through case B binary evolution. Van Bever & Vanbeveren (1997) found that a minority of the Be stars (less than 20% and possibly as low as 5%) are due to close binary interaction. Our results show that, combining the effects of both mass transfer and merger, the fraction of Be stars in B type stars can reach  $\sim 13\% - 30\%$ , compatible with the observational results of 20% – 30% (Zorec & Briot 1997) and  $1/5 - 1/3$  (McSwain & Gies 2005). We emphasize that all the numbers of Be stars cited in this work should be taken as upper limits, because not all rapidly rotating B type stars exhibit the Be phenomenon.

Finally we summarize our results as follows.

(1) By considering different possible mass accretion histories for the mass gainer in a binary, we calculate the critical mass ratios for stable mass transfer. We find that in Be/NS binaries the Be star masses and orbital periods are consistent with observations if they are formed by stable and nonconservative mass transfer (i.e., channel 1 of Model II).

(2) There are about  $10^6$  isolated Be stars in the Galaxy originating from both disrupted Be/NS systems and mergers of two MS stars, but the latter play a much more important role.

(3) The ratio of Be/NS binaries to the ones with BHs can be as small as  $\sim 7$ , suggesting that there could exist a hidden population of Be/BH binaries in the Galaxy.

(4) Both Be/He and Be/WD binaries tend to have low-mass Be stars and orbital periods of tens of days. Most of the He stars in Be/He binaries are less massive than  $\sim 2.5M_{\odot}$ .

(5) The fraction of Be stars resulting from binary evolution among B type stars is around 13% – 30%.

We thank the referee for constructive comments which have greatly helped improve the

manuscript. This work was supported by the Natural Science Foundation of China under grant numbers 11133001, 11203009 and 11333004, the Strategic Priority Research Program of CAS (under grant number XDB09000000), and the graduate innovative project of Jiangsu Province (CXZZ13-0043).

### A. Two Cases of Evolutionary Sequences

To illustrate how the stability of mass transfer depends on the evolutionary state of the binary system, in Fig. A1 we show the evolutionary tracks of a binary in Model I with the initial parameters of  $M_1 = 10M_\odot$  and  $q = 3$ . Prior to the mass transfer, the primary has lost some of its mass in a stellar wind, leading to a slight widening of the orbit. In the top panel, the initial orbital period  $P_{\text{orb}}$  is set to be 3 days. At an age  $\sim 22.16$  Myr, the primary, still on the MS, overfills its RL and commences mass transfer. The orbital period decreases from 3.2 day to 2 days after  $\sim 1M_\odot$  mass has been transferred to the secondary. Meanwhile, the mass transfer rate rises to  $\sim 10^{-3}M_\odot \text{ yr}^{-1}$ . At this time the radius of the secondary exceeds its RL radius and the binary becomes contact. In the middle panel, the initial  $P_{\text{orb}}$  is taken to be 15 days. The primary has evolved off the MS and entered the shell-burning phase when RLOF initiates. The mass transfer proceeds rapidly but stably at a rate  $\sim 10^{-4} - 10^{-2}M_\odot \text{ yr}^{-1}$ . A small amount ( $\sim 0.4M_\odot$ ) of the transferred material is able to spin up the secondary into a Be star, and the rest of the material is assumed to be ejected out of the system. The orbital period decreases until the primary's mass drops to  $\sim 5M_\odot$ . After that the mass ratio reverses, and  $P_{\text{orb}}$  increases to  $\sim 13$  days at the end of the evolution. After the envelope of the primary is stripped, a  $\sim 2M_\odot$  He core is left. In the bottom panel, the initial  $P_{\text{orb}}$  is 320 days. When the primary overfills its RL, it has climbed to the red giant branch. Once RLOF starts, the mass transfer rate rises to  $\sim 10^{-2}M_\odot \text{ yr}^{-1}$  within  $\lesssim 100$  yr. The mass transfer proceeds on the dynamical timescale and a subsequent spiral-in stage is followed.

In Fig. A2 we present similar evolutionary sequences for a binary in Model II with  $M_1 = 10M_\odot$  and  $q = 2$ . The initial  $P_{\text{orb}}$  are 2, 3, and 5 days in the top, middle and bottom panels, respectively. In the top panel, at the onset of RLOF (at an age of  $\sim 18.86$  Myr), the primary is in the MS stage. When the orbital period decreases to less than  $\sim 1.6$  days and the mass transfer rate increases to  $\gtrsim 10^{-4}M_\odot \text{ yr}^{-1}$ , the secondary fills its RL, leading to a contact phase. In the middle panel, the mass exchange begins at an age  $\sim 21.86$  Myr when the primary is also a MS star. The binary experiences stable mass transfer at a rate  $\sim 10^{-5} - 10^{-3}M_\odot \text{ yr}^{-1}$ , with a temporary phase of detachment. Half of the transferred material is ejected from the binary, so the secondary accretes  $\sim 4M_\odot$  mass. The resulting

binary consists of a  $2 M_{\odot}$  He star and a  $\sim 9 M_{\odot}$  Be star. In the bottom panel, RLOF occurs (at an age  $\sim 23.53$  Myr) when the primary has evolved to the HG. The mass transfer rate increases to  $\sim 10^{-3} M_{\odot} \text{yr}^{-1}$  and the orbit shrinks to less than 4 days. The secondary quickly fills its RL followed by a CE phase.

## REFERENCES

- Apparao, K. M. V. 1991, *A&A*, 248, 139
- Artymowicz, P. & Lubow, S. H. 1994, *ApJ*, 421, 651
- Belczynski, K., Kalogera, V., Rasio, F., Taam, R., Zezas, A. et al. 2008, *ApJS*, 174, 223
- Belczynski, K. & Ziolkowski, J. 2009, *ApJ*, 707, 870
- Carciofi, A. C., Okazaki, A. T., Le Bouquin, J.-B., et al. 2009, *A&A*, 504, 915
- Casares, J., Negueruela, I. et al. 2014, *Nature*, 505, 378
- Cheng, Z.-Q., Shao, Y., & Li, X.-D. 2014, *ApJ*, 786, 128
- de Jager, C., Nieuwenhuijzen, H., & van der Hucht, K. A. 1988, *A&A*, 72, 259
- de Kool, M. 1990, *ApJ*, 358, 189
- de Mink, S. E., Pols, O. R., & Hilditch, R. W. 2007, *A&A*, 467, 1181
- de Mink, S. E., Pols, O. R., Langer, N., & Izzard, R. G. 2009, *A&A*, 507, L1
- de Mink, S. E., Langer, N., Izzard, R. G., Sana, H., & de Koter, A. 2013, *ApJ*, 764, 166
- Derviřođlu, A., Tout, C. A., & Ibañođlu, C. 2010, *MNRAS*, 406, 1071
- Deschamps, R., Siess, L., Davis, P. j., & Jorissen, A. 2013, *A&A*, 557, A40
- Dessart, L., Burrows, A., Ott, C. D., Livne, E., Yoon, S.-C., & Langer, N. 2006, *ApJ*, 644, 1063
- Dewi, J. & Tauris, T. 2000, *A&A*, 360, 1043
- Eggleton, P. P. 1971, *MNRAS*, 151, 351
- Eggleton, P. P. 1972, *MNRAS*, 156, 361

- Eggleton, P. P. 1983, *ApJ*, 268, 368
- Ekström, S., Meynet, G., Maeder, A., & Barblan, F. 2008, *A&A*, 478, 467
- Farr, W. M., Sravan, N., Cantrell, A., et al. 2011, *ApJ*, 741, 103
- Fryer, C., Belczynski, K., Wiktorowicz, G., Dominik, M., Kalogera, V., & Holz, D. 2012, *ApJ*, 749, 91
- Ge, H., Hjellming, M. S., Webbink, R. F., Chen, X., & Han, Z. 2010, *ApJ*, 717, 724
- Han, Z., Podsiadlowski, P., Maxted, P. F. L., Marsh, T. R., & Ivanova, N. 2002, *MNRAS*, 336, 449
- Habets, G., & Heintze, J., 1981, *A&AS*, 46, 193
- Hobbs, G., Lorimer, D. R., Lyne, A. G., & Kramer, M. 2005, *MNRAS*, 360, 974
- Huang, W., Gies, D. R., & McSwain, M. V. 2010, *ApJ*, 722, 605
- Hurley, J. R., Pols, O. R., & Tout, C. A. 2000, *MNRAS*, 315, 543
- Hurley, J. R., Tout, C. A., & Pols, O. R. 2002, *MNRAS*, 329, 897
- Hut, P. 1981, *A&A*, 99, 126
- Ivanova, N. & Taam, R. E. 2004, *ApJ*, 601, 1058
- Jiang, D., Han, Z., Yang, L., & Li, L. 2013, *MNRAS*, 428, 1218
- Jones, C. E., Molak, A., Sigut, T. A. A., et al. 2009, *MNRAS*, 392, 383
- Kahabka, P., Haberl, F., Payne, J. L., & Filipović, M. D. 2006, *A&A*, 458, 285
- Kalogera, V. & Webbink, R. F. 1996, *ApJ*, 458, 301
- Kiel, P. D. & Hurley, J. R. 2006, *MNRAS*, 369, 1152
- King, A. R. 1988, *QJRAS*, 29, 1
- Kochanek, C. S. 2014, *ApJ*, 785, 28
- Knigge, C., Coe, M. J., & Podsiadlowski, Ph. 2011, *Nat*, 479, 372
- Kroupa, P., Tout, C. A., & Gilmore, G. 1993, *MNRAS*, 262, 545
- Lee, U., Osaki, Y., & Saio, H. 1991, *MNRAS*, 250, 432

- Li, K. J., Kong, A. K. H., & Charles, P. A. 2012, *ApJ*, 761, L99
- Li, X.-D. & van den Heuvel, E. P. J. 1997, *A&A*, 322, L9
- Liu, Q. Z., van Paradijs, J., & van den Heuvel, E. P. J. 2006, *A&A*, 455, 1165
- Lombardi, J. C., Jr., Rasio, F. A., & Shapiro, S. L. 1995, *ApJL*, 445, L117
- Lubow, S. H. & Shu, F. H. 1975, *ApJ*, 198, 383
- McBride, V., Coe, M., Negueruela, I., Schurch, M., & McGowan, K. 2008, *MNRAS*, 388, 1198
- McGill, M. A., Sigut, T. A. A., & Jones, C. E. 2013, *ApJS*, 204, 2
- McSwain, M. V., & Gies, D. R. 2005, *ApJS*, 161, 118
- Munar-Adrover, P., Paredes, J. M., Ribó, M. et al. 2014, *ApJ*, 786, L11
- Negueruela I. 1998, *A&A*, 338, 505
- Negueruela, I. & Okazaki, A. T. 2001, *A&A*, 369, 108
- Nelson, C. A. & Eggleton, P. P. 2001, *ApJ*, 552, 664
- Nielsen, M. T. B., Dominik, C., Nelemans, G. & Voss, R. 2013, *A&A*, 549, A32
- Neo, S., Miyaji, S., Nomoto, K., & Sugimoto, D. 1977, *PASJ*, 29, 249
- Okazaki, A. T. 2001, *PASJ*, 53, 119
- Özel, F., Psaltis, D., Narayan, R., & McClintock, J. E. 2010, *ApJ*, 725, 1918
- Packet, W., 1981, *A&A*, 102, 17
- Paczynski, B. 1991, *ApJ*, 370, 597
- Pejcha, O. & Thompson, T. A. 2014, *ApJ*, in press (arXiv:1409.0540)
- Petrovic, J., Langer, N., & van der Hucht, K. A. 2005, *A&A*, 435, 1013
- Podsiadlowski, P., Joss, P. C., & Hsu, J. J. L. 1992, *ApJ*, 391, 246
- Podsiadlowski, Ph., Rappaport, S., & Pfahl, E. D. 2002, *ApJ*, 565, 1107
- Pols, O. R., Coté, J., Waters, L. B. F. M., & Heise, J. 1991, *A&A*, 241, 419

- Pols, O. R. & Marinus, M. 1994, *A&A*, 288, 475
- Pols, O. R., Tout, C. A., Eggleton, P. P., & Han Z. 1995, *MNRAS*, 274, 964
- Popham, R., & Narayan, R. 1991, *ApJ*, 370, 604
- Portegies Zwart, S. F. 1995, *A&A*, 296, 691
- Porter, J. M., & Rivinius, T. 2003, *PASP*, 115, 1153
- Raguzova, N. V. 2001, *A&A*, 367, 848
- Raguzova, N. V. & Lipunov, V. M. 1998, *A&A*, 340, 85
- Rappaport, S., & van den Heuvel, E. 1982, in *Proc. IAU Symp. 92, Be stars*, ed. M. Jасhek & H. G. Groth (Dordrecht: Reidel), 327
- Reig, P. 2011, *Ap&SS*, 332, 1
- Sana, H., de Mink, S. E., de Koter, A., et al. 2012, *Science*, 337, 444
- Schröder, K., Pols, O. R., & Eggleton, P. P. 1997, *MNRAS*, 285, 696
- Shao, Y. & Li, X.-D. 2012, *ApJ*, 756, 85
- Shu, F. H. & Lubow, S. H. 1981, *ARA&A*, 19, 277
- Sigut, T. A. A., McGill, M. A., & Jones, C. E. 2009, *ApJ*, 699, 1973
- Slettebak A., 1982, *ApJS*, 50, 55
- Soberman, G. E., Phinney, E. S., & van den Heuvel, E. P. J. 1997, *A&A*, 327, 620
- Stancliffe, R. & Eldridge, J. 2009, *MNRAS*, 396, 1699
- Sturm, R., Harbel, F., Pietsch, W. et al. 2012, *A&A*, 537, A76
- Tassoul, J.-L. 1987, *ApJ*, 322, 856
- Tauris, T. M., van den Heuvel, E. P. J., & Savonije, G. J. 2000, *ApJ*, 530, L93
- Ulrich, R. K., & Burger, H. L. 1976, *ApJ*, 206, 509
- Van Bever, J. & Vanbeveren, D. 1997, *A&A*, 322, 116
- van den Heuvel, E., & Rappaport, S. 1987, in *Proc. IAU Coll. 92, Physics of Be Stars*, ed. A. Slettebak & T. P. Snow (Cambridge: Cambridge Univ. Press), 291

- Wade, G. A., Grunhut, J. H., & MiMeS Collaboration, 2012, ASP Conference Proceedings, Vol. 464, ed. A. Carciofi and Th. Rivinius (San Francisco: Astronomical Society of the Pacific), 405
- Webbink, R. F. 1984, ApJ, 277, 355
- Wheeler, J. C. & Pooley, D. 2013, ApJ, 762, 75
- Wood, K., Bjorkman, K. S., & Bjorkman, J. E. 1997, ApJ, 477, 926
- Woods, T. E., Ivanova, N., van der Sluys, M. V. & Chaichenets, S. 2012, ApJ, 744, 12
- Woosley, S. E., Heger, A., & Weaver, T. A. 2002, Rev. Mod. Phys., 74, 1015
- Xu, X.-J. & Li, X.-D., 2010, ApJ, 716, 114
- Yakut, K. & Eggleton, P. P. 2005 ApJ, 629, 1055
- Zahn J.-P. 1977, A&A, 57, 383
- Zhang, F., Li, X.-D., & Wang, Z.-R. 2004, ApJ, 603, 663
- Zorec, J. & Briot, D. 1997, A&A, 318, 443

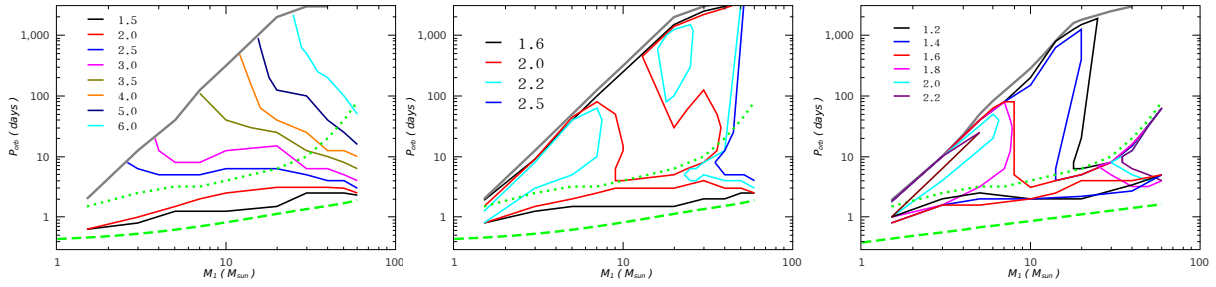


Fig. 1.— The solid curves describe the allowed parameter space in the initial  $P_{\text{orb}} - M_1$  plane for stable mass transfer, in which contact and CE phases can be avoided. The left, middle and right panels correspond to Models I, II and III, respectively. In each panel, the number next to each colored label denotes the initial mass ratio ( $q = M_1/M_2$ ) of the binary components. The green dashed, green dotted and black solid curves represent the orbital periods when the primary overflows its RL at ZAMS, the end of MS, and the end of HG, respectively (they depend very weakly on  $q$ , and here we adopt  $q = 2$ ).

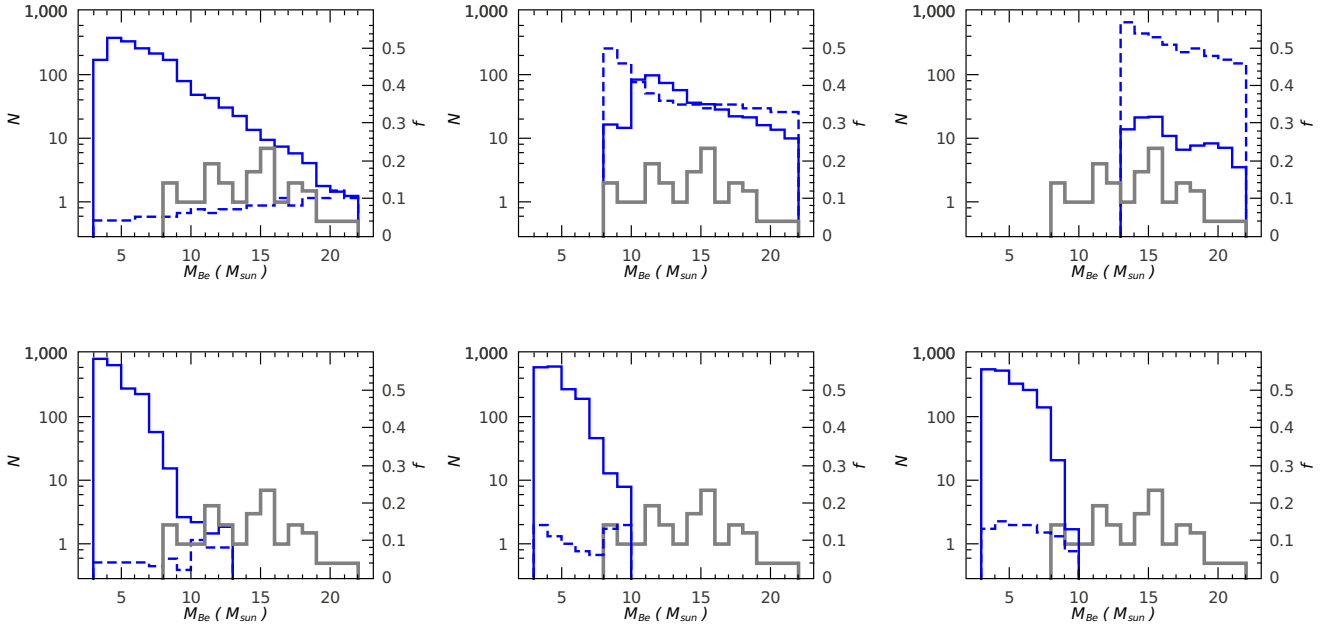


Fig. 2.— The blue solid lines represent the mass distributions of Be stars in Be/NS binaries formed through channels 1 (top panel) and 2 (bottom panel). The left, middle and right panels correspond to Models I, II and III, respectively. The blue dashed lines reflect the fraction  $f$  of the average accreted mass by the Be stars in each bin. The grey dashed lines show the observational distribution of Be stars with a NS companion. Here the spectral type data of Be stars are taken from Reig (2011). We calibrate the relation between the spectral types and the masses from Habets & Heintze (1981).

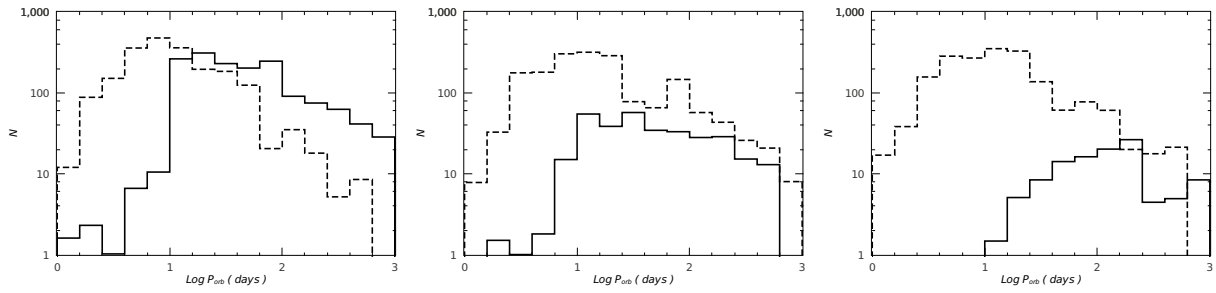


Fig. 3.— The distributions of the orbital periods of Be/NS binaries. The solid and dashed curves correspond to the systems formed through channels 1 and 2, respectively. The left, middle and right panels correspond to Models I, II and III, respectively.

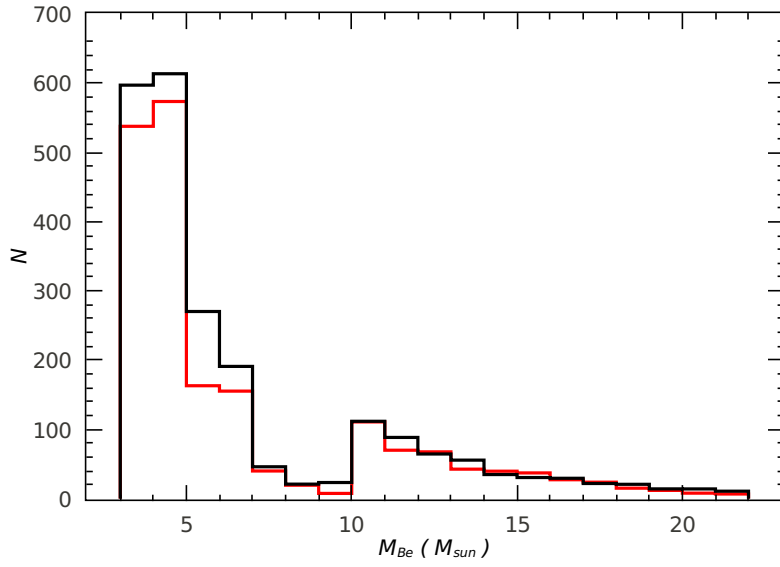


Fig. 4.— The distributions of the masses of Be stars in Be/NS systems in the standard model. The black and red curves correspond to the parameter  $V_{\text{eq}}/V_{\text{crit}} = 0.8$  and  $0.95$ , respectively .

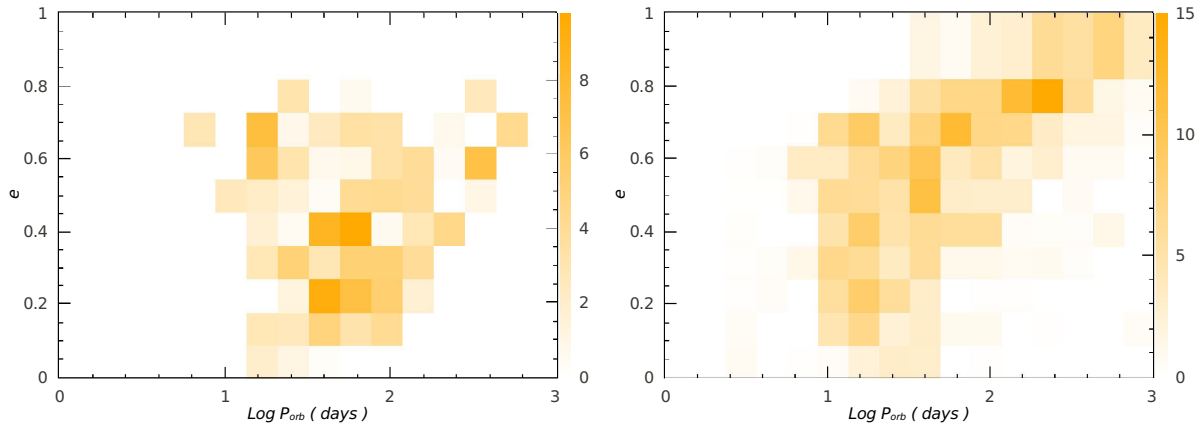


Fig. 5.— The distribution of Be/NS binaries in the  $P_{\text{orb}} - e$  plane, formed in the standard model. In the left and right panels the NSs originate from electron-capture SNe and core-collapse SNe, respectively.

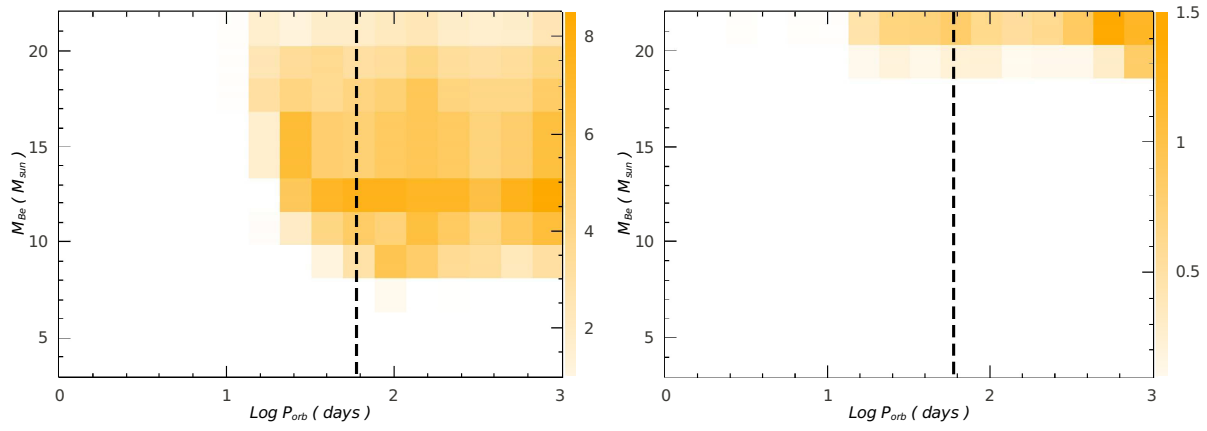


Fig. 6.— The distribution of Be/BH binaries in the  $P_{orb} - M_{Be}$  plane in Models I (left panel) and II (right panel). The dashed line shows the orbital period of the Be/BH binary MWC 656.

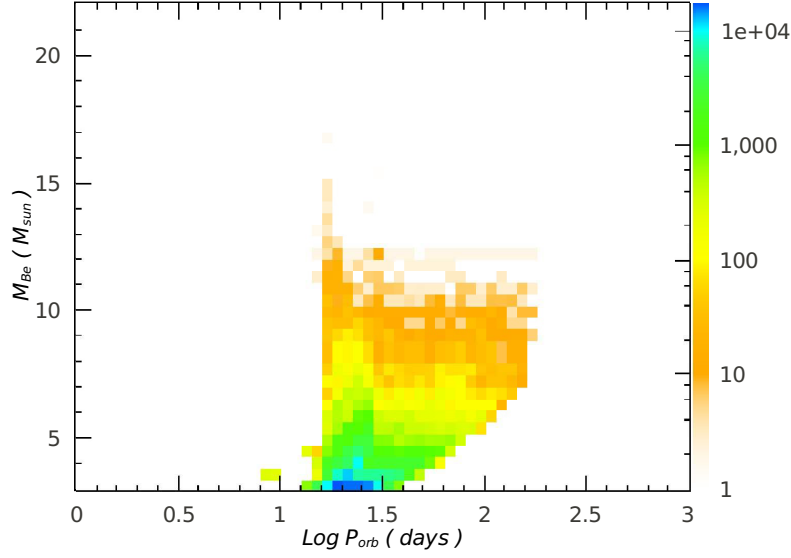


Fig. 7.— The distribution of Be/He binaries in the  $P_{\text{orb}} - M_{\text{Be}}$  plane in the standard model.

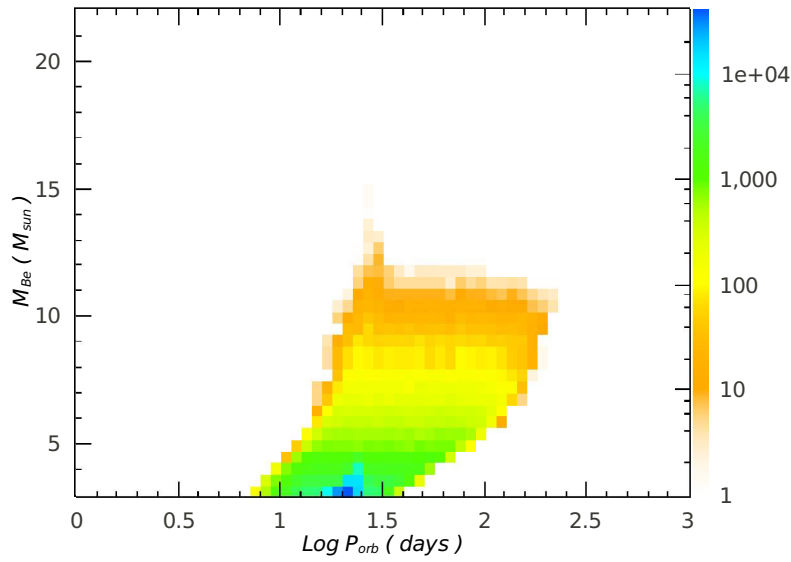


Fig. 8.— Same as Fig. 7, but for Be/WD binaries.

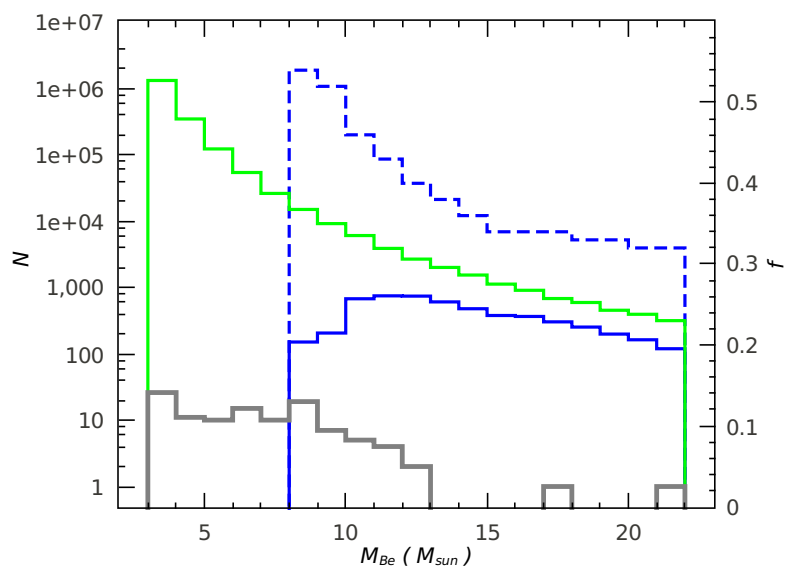


Fig. 9.— The blue and green solid lines represent the mass distribution of isolated Be stars evolved from disrupted Be/NS binaries and mergers of two MS stars in the standard model, respectively. The blue dashed line denotes the fraction  $f$  of average accreted mass by the Be stars in each bin in the first case. Observational distribution of isolated Be stars is shown in the grey line, with the spectral type data of Be stars taken from Slettebak (1982).

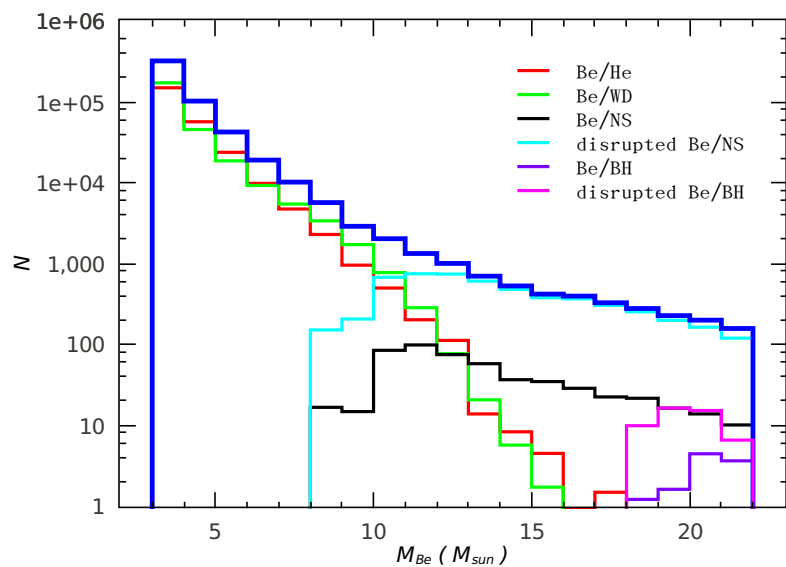


Fig. 10.— The mass distribution of all Be stars evolved from the standard model, shown in the blue line. Other **six** lines represent the distributions of Be stars in Be/He, Be/WD, Be/NS, and Be/BH binaries, and isolated Be stars from disrupted Be/NS and Be/BH systems.

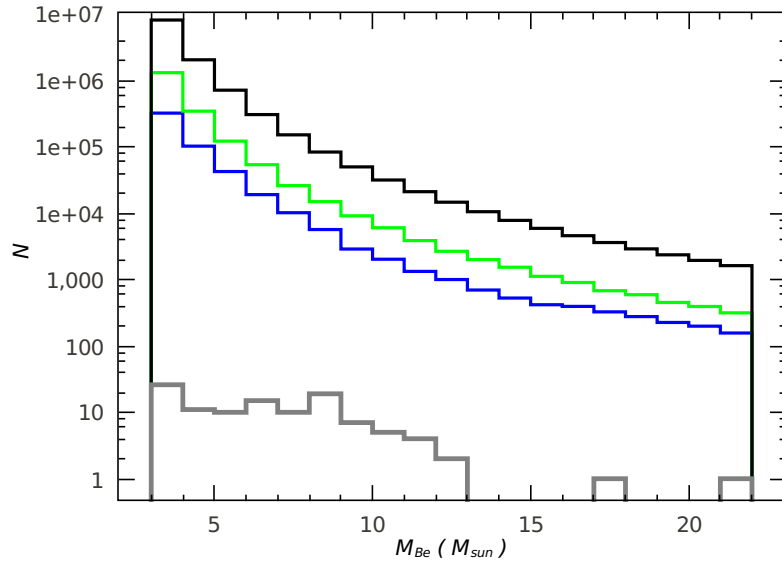


Fig. 11.— The black, blue, and green lines represent the mass distributions of all B type stars, Be stars formed from channel 1 and from MS mergers in the standard model, respectively. The grey line shows the observational distribution of isolated Be stars in the Galaxy.

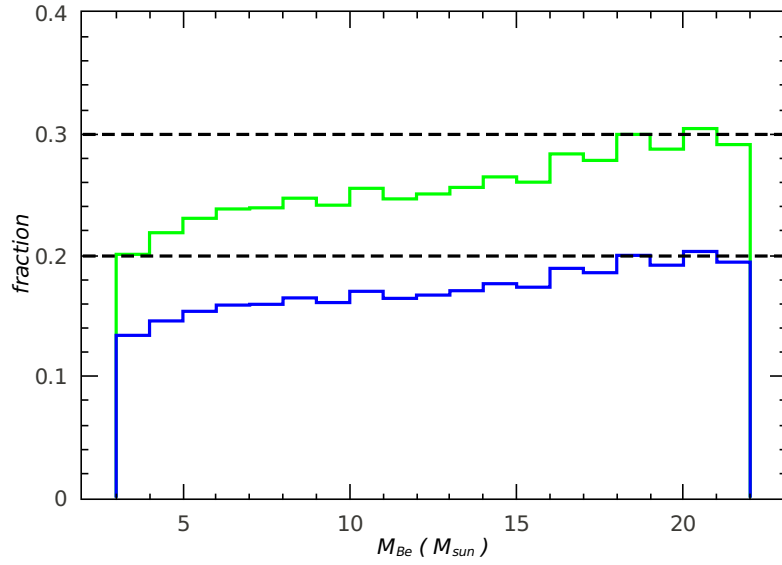


Fig. 12.— The fraction of Be stars in B type stars. The green and blue solid lines are obtained under the assumption that the fraction of primordial binaries in the Galaxy are 100% and 50%, respectively. The two dashed lines show the range of derived fractions from observations (Zorec & Briot 1997).

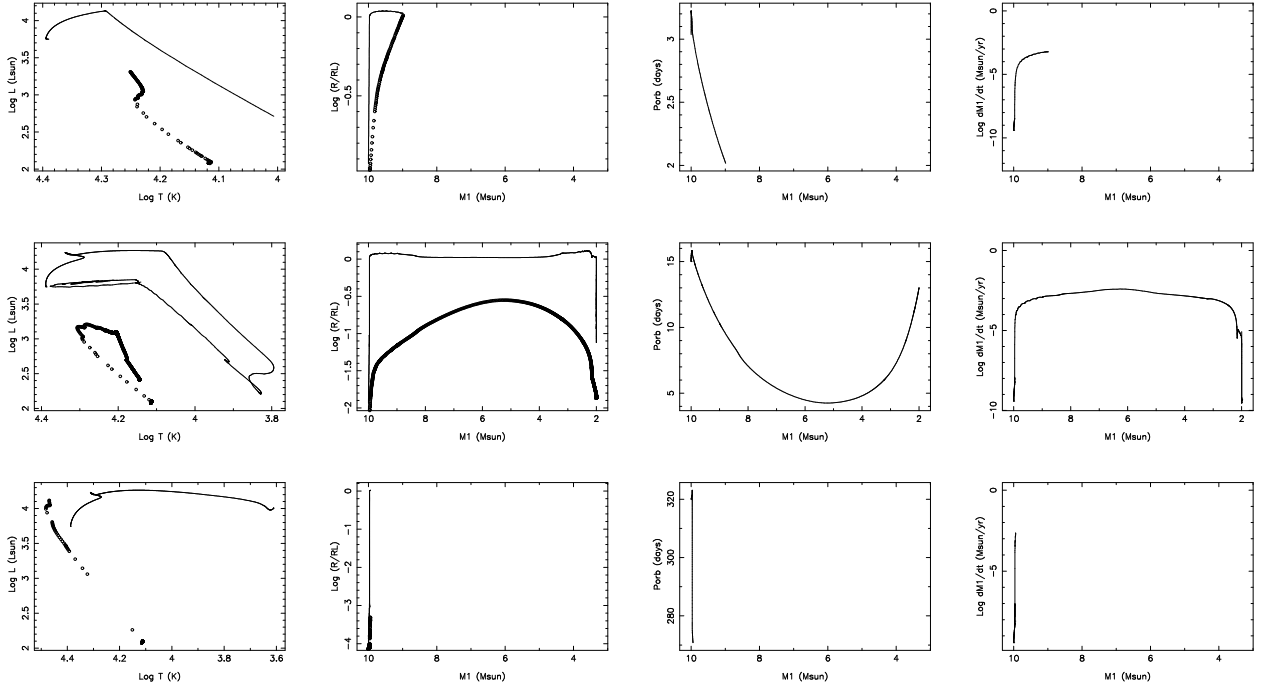


Fig. A1.— Evolution of the binary systems with  $M_1 = 10M_\odot$ ,  $q = 3$ , and  $P_{\text{orb}} = 3$  day (top), 15 days (middle), and 320 days (bottom) in Model I. Panels from left to right are shown the evolutionary tracks of the primary (**solid curve**) and the secondary (**dotted curve**) in the H-R diagram, the ratios of the primary (solid curve) and secondary (dotted curve) radii to their RL radii, the orbital period, and the mass transfer rate.

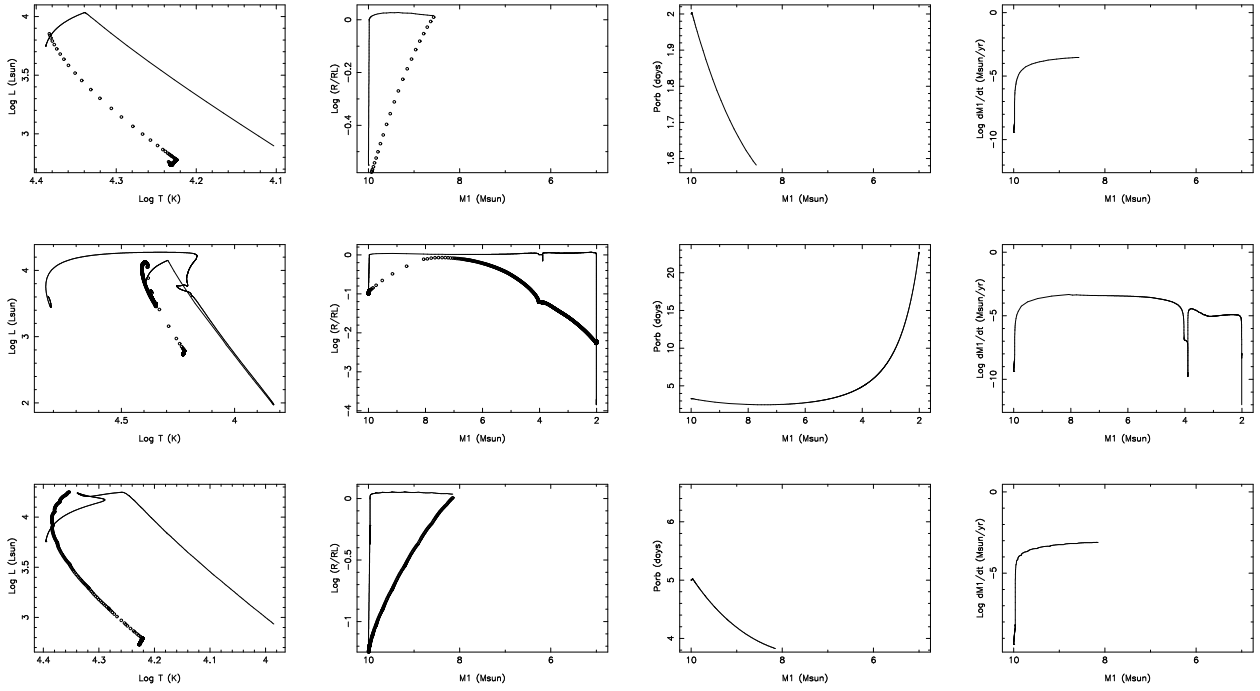


Fig. A2.— Same as Fig. A1, but for binary systems with  $q = 2$  and  $P_{\text{orb}} = 2$  days (top), 3 days (middle), and 5 days (bottom) in Model II.

Table 1: The predicted numbers of Be/He, Be/WD, Be/NS, and Be/BH binaries and isolated Be stars from disrupted Be/NS, Be/BH binaries, and MS star mergers in the Galaxy in the three models and the two different channels.

Models	I	I	II	II	III	III
Channels	1	2	1	2	1	2
$N_{\text{BeHe}}$	$6.5 \times 10^4$	$< 100$	$2.5 \times 10^5$	$< 100$	$4.1 \times 10^5$	$< 100$
$N_{\text{BeWD}}$	$1.8 \times 10^5$	$1.3 \times 10^5$	$2.6 \times 10^5$	$1.4 \times 10^5$	$1.3 \times 10^5$	$1.6 \times 10^5$
$N_{\text{BeNS}}$	1800	2043	531	1761	102	1842
$N_{\text{dBeNS}}$	$2.0 \times 10^4$	3930	5246	2450	1964	2505
$N_{\text{BeBH}}$	245	$< 1$	10	$< 1$	0	$< 1$
$N_{\text{dBeBH}}$	573	$< 1$	51	$< 1$	0	$< 1$
$N_{\text{merger}}$	$1.6 \times 10^6$	0	$1.9 \times 10^6$	0	$2.1 \times 10^6$	0